THE EFFECT OF A PLANE BOUNDARY ON WAVE INDUCED FORCES ACTING ON A SUBMERGED CYLINDER

Houston Keith Jones

NAVAL POSTGRADUATE SCHOOL
Monterey, California

THESIS

THE EFFECT OF A PLANE BOUNDARY ON WAVE INDUCED FORCES ACTING ON A SUBMERGED CYLINDER

by

Houston Keith Jones

June 1975

Thesis Advisor: T. Sarpkaya

SECURITY CLASSIFICATION OF THIS PAGE (When Data Entered)

REPORT DOCUMENTATION PAGE

READ INSTRUCTIONS BEFORE COMPLETING FORM

1. REPORT NUMBER	2. GOVT ACCESSION NO.
3. RECIPIENT'S CATALOG NUMBER	
4. TITLE (and Subtitle) The Effect of a Plane Boundary on Wave Induced Forces Acting on a Submerged Cylinder	5. TYPE OF REPORT & PERIOD COVERED Master's Thesis Thesis
	6. PERFORMING ORG. REPORT NUMBER
7. AUTHOR(s) Houston Keith Jones	8. CONTRACT OR GRANT NUMBER(s)
9. PERFORMING ORGANIZATION NAME AND ADDRESS Naval Postgraduate School Monterey, California 93940	10. PROGRAM ELEMENT, PROJECT, TASK AREA & WORK UNIT NUMBERS
11. CONTROLLING OFFICE NAME AND ADDRESS Naval Postgraduate School Monterey, California 93940	12. REPORT DATE June 1975
	13. NUMBER OF PAGES
14. MONITORING AGENCY NAME & ADDRESS (if different from Controlling Office) Naval Postgraduate School Monterey, California 93940	15. SECURITY CLASS. (of this report) Unclassified
	15a. DECLASSIFICATION/DOWNGRADING SCHEDULE

16. DISTRIBUTION STATEMENT (of this Report)

Approved for public release; distribution unlimited.

17. DISTRIBUTION STATEMENT (of the abstract entered in Block 20, if different from Report)

18. SUPPLEMENTARY NOTES

19. KEY WORDS (Continue on reverse side if necessary and identify by block number)

20. ABSTRACT (Continue on reverse side if necessary and identify by block number)

The in-line and transverse forces acting on cylinders of 1.0 inch to 2.5 inches diameter placed near a plane wall in a harmonically oscillating flow have been measured. The drag and inertia coefficients C_d and C_m for the in-line force and the lift coefficients C_{lA} and C_{lT} for the transverse forces away and

toward the wall, respectively, have been determined as a function of the relative gap e/D between the wall and the cylinder and the period parameter $V_m T/D$. The relative gap ranged from 0.0143 to unity and the period parameter from zero to 35. In the subcritical range where these experiments have been performed, the effect of the Reynolds number, which ranged from 4,000 to 30,000, was found to be secondary and certainly obscured by the excellent correlation provided by the period parameter.

The frequency of the transverse force was found to range from one to five times the frequency of oscillation of the harmonic motion, but a dominant frequency of twice the oscillation frequency was seen over most of the values of $V_m T/D$.

The Effect of a Plane Boundary on Wave

Induced Forces Acting on a Submerged Cylinder

by

Houston Keith Jones
Ensign, United States Navy
B.S., United States Naval Academy, 1974

Submitted in partial fulfillment of the
requirements for the degree of

MASTER OF SCIENCE IN OCEANOGRAPHY

from the

NAVAL POSTGRADUATE SCHOOL
June 1975

ABSTRACT

The in-line and transverse forces acting on cylinders of 1.0 inch to 2.5 inches diameter placed near a plane wall in a harmonically oscillating flow have been measured. The drag and inertia coefficients C_d and C_m for the in-line force and the lift coefficients C_{lA} and C_{lT} for the transverse forces away and toward the wall, respectively, have been determined as a function of the relative gap e/D between the wall and the cylinder and the period parameter V_mT/D. The relative gap ranged from 0.0143 to unity and the period parameter from zero to 35. In the subcritical range where these experiments have been performed, the effect of the Reynolds number, which ranged from 4,000 to 30,000, was found to be secondary and certainly obscured by the excellent correlation provided by the period parameter.

The frequency of the transverse force was found to range from one to five times the frequency of oscillation of the harmonic motion, but a dominant frequency of twice the oscillation frequency was seen over most of the values of V_mT/D.

TABLE OF CONTENTS

LIST OF FIGURES

NOMENCLATURE

A	amplitude of the motion
C_d	average drag coefficient
C_{lA}	maximum lift coefficient away from the boundary
C_{lT}	maximum lift coefficient toward the boundary
C_m	average inertia coefficient
D	diameter of test cylinder
e	normal distance between the boundary and the cylinder surface
F	instantaneous total force acting on the test cylinder
F_d	drag force acting on the test cylinder
F_l	lift force acting on the test cylinder
h	water depth
k	wave number $(2\pi/l)$
L	length of test cylinder
l	wave length
T	period of oscillation
t	time
u	horizontal fluid particle velocity
V	instantaneous velocity
V_m	maximum velocity
w	vertical fluid particle velocity
z	vertical position of the test cylinder
λ	percent error
ν	fluid kinematic viscosity
ρ	fluid density
σ	wave frequency $(2\pi/T)$

ACKNOWLEDGEMENTS

This project has been carried out under the direction of Professor T. Sarpkaya. I would like to express my sincere gratitude for his guidance, but especially for the knowledge he imparted to me. Appreciation is also extended to Professor E. Thornton for his assistance in completing this thesis and Doctor D. F. Leiper for his time spent to read it.

I. INTRODUCTION

A. EXPERIMENTAL JUSTIFICATION

With the current energy deficit becoming of vital importance, offshore oil production assumed great priority, and pipe lines became the most feasible mode of liquid transportation to the shore. This, in turn, necessitated the determination of the wave and/or current induced forces on submerged pipes placed at or near the ocean bottom. The problem, however, is not unique to the pipe lines.

Underwater cables for communication and sensing purposes and all submerged structures, be they offshore oil platforms or oceanographic research instruments, are subjected to wave induced forces.

The proximity of pipe to a solid boundary, such as the ocean bottom, further complicates the problem, and, unless the submerged pipe lines are anchored to a buoy system or buried, the bottom effects must also be considered. Even buried pipe lines, subject to scouring can become uncovered and have their support dug out from under, leaving them sensitive to wave induced forces.

B. BACKGROUND THEORY

The in-line force acting on a cylinder immersed in a time-invariant flow may be expressed, according to Morison and his co-workers [6] as:

$$F=F_d+F_m= 1/2LC_dD\rho V^2+C_m\pi D^2/4\ LdV/dT \qquad (1)$$

in which C_d and C_m represent time-invariant drag and inertia coefficients, respectively. The first term on the right-hand side of this equation represents the velocity-squared dependent drag force and the second term the acceleration-dependent inertia force.

A simple dimensional analysis shows that the time-averaged drag and inertia coefficients for a cylinder immersed in a harmonically oscillating uniform flow, represented by

$$V=-V_m\cos 2\pi t/T$$

depend on the period parameter V_mT/D and the Reynolds number V_mD/ν. In addition to the in-line force, the cylinder is subjected to an alternating transverse force due to separation and vortex shedding. The proximity of a solid boundary can alter significantly the magnitudes of both the in-line and transverse forces and requires the determination of the wall proximity effect on the drag, inertia, and lift coefficients. In fact, it is the determination of this effect that prompted the present study.

A harmonically oscillating uniform flow represents only approximately the oscillatory motion induced by waves about a submerged cylinder. Nevertheless, the wave-induced forces may be predicted with sufficient accuracy through the use of drag, inertia, and the lift coefficients obtained with harmonic flow, provided that the velocities and accelerations

about the cylinder are either measured or calculated through the use of an appropriate wave theory.

For small amplitude waves, Airy's theory may be used to evaluate the velocities and accelerations of a given time and depth. The limitations of this theory are well-known and will not be represented here.

The horizontal and vertical components of velocity may be written as [11],

$$u=A\sigma(\cosh k(h+z)/\sinh kh)\cos\theta \tag{2}$$

$$w=A\sigma(\sinh k(h+z)/\sinh kh)\sin\theta \tag{3}$$

in which A represents the wave amplitude, k the wave number defined by $2\pi/l$, h the water depth, z the vertical position of the cylinder, σ the wave frequency given by $\frac{2\pi}{T}$ and $\theta=kx-\sigma t$.

The components of acceleration are given by

$$\delta u/\delta t=-A\sigma^2(\cosh k(h+z)/\sinh kh)\sin\theta \tag{4}$$

$$\delta w/\delta t=A\sigma^2(\sinh k(h+z)/\sinh kh)\cos\theta \tag{5}$$

The in-line force may be expressed through the combination of equations (1), (2), and (4) to yield,

$$F=A\sigma^2 LC_m \frac{D^2}{4}\frac{\cosh k(h+z)}{\sinh kh}\sin\theta$$

$$-A^2 C_d L\rho D\frac{(\cosh k(h+z))^2}{(\sinh kh)^2}|\cos\sigma t|\cos\sigma t \tag{6}$$

The transverse force cannot, however, be calculated in a similar manner through the use of equations (1), (3), and (5).

It is fundamentally the eddy behavior that determines the transverse force. Thus, the lift resulting from a nonlinear motion is not susceptible to estimation by superposition of individual responses to each harmonic acting in isolation.

The lift coefficients in the present study are evaluated as follows:

$$C_{1A} = \frac{(\text{maximum transverse force away from the wall in a cycle})}{0.5\rho D L V_m^2} \tag{7}$$

$$C_{1T} = \frac{(\text{maximum transverse force toward the wall in a cycle})}{0.5\rho D L V_m^2} \tag{8}$$

Force coefficients based on other time-invariant magnitudes such as the root-square values could have been easily obtained. It will suffice here to remark that a simple Fourier analysis for the in-line force and the peak value for the transverse force proved adequate for all purposes.

The determination of the coefficients C_d, C_m, C_{1A}, C_{1T} constitute the essence of the present study for a cylinder placed within the proximity of a plane wall in a harmonically oscillating flow.

C. RELATED RESEARCH

Yamamoto, et al., in 1974, studied wave forces on cylinders near a plane boundary in the range of Reynolds numbers from 2,000 to 30,000 and the surface period parameter from about 0.3 to 3. The total force was considered as the sum of components due to water particle velocity squared (lift and

drag forces), and due to water particle acceleration (inertia force). They have correlated the force coefficients C_l and C_d with the relative distance of the cylinder from the boundary.

The vertical and horizontal hydrodynamic forces were obtained for unseparated flow over the submerged cylinder by using the method of double images and applying Blasius' theorum.

The results indicated that the proximity of a plane boundary modified both the lift and the inertia coefficients. However, these results are applicable only to unseparated flows where drag is negligible compared to inertial forces. Within a narrow range and relatively low values of the period parameter, it was shown that the maximum horizontal force occurred at zero crossings of the surface wave, indicating that wake dependent drag force is negligible and the horizontal force is composed mainly of the inertia force. The vertical force, for larger values of the relative distance was unsinusoidal with large downward forces (toward boundary) at the surface wave crests and small upward forces at surface troughs.

In 1967, a theory for simple shear flow across a circular cylinder in proximity to a plane wall, was developed by Arie and Kiya [2]. Theoretically, they showed that a force acts downward (negative uplift) for uniform velocity, but a force acting upwards (away from the plane) exists for flow having a velocity gradient. Their experimental data failed to enforce

this theory, but did show that lift on the cylinder increased as the clearance between the cylinder and wall decreased. A wind tunnel was used for their experimentation.

Studies on the effects of ocean currents on pipes anchored just above the ocean floor were conducted by Wilson and Caldwell [12] in 1970, and the lift and drag coefficients were determined. The frequency of the forces on the pipe was found to be effected by the eddy-shedding frequencies.

In 1971, a study by Grace [3] on the effect of the clearance of pipe above a flume and the effect of orientation of the pipe to the wave crest was made. With clearance ranges from 1/32 inch to 1-1/2 inches and wave periods of 2 to 6 seconds in 3 foot deep water, he found that the horizontal force normal to the pipe was not effected by bottom clearance and that this force decreased as the pipe became perpendicular to the wave fronts. He also found that the "vertical force" decreased as the bottom clearance decreased.

In much of the work conducted on wave forces, correlations between C_m, C_d, and the Reynolds number $V_m D/\nu$, where ν is the kinematic viscosity, have been sought with little success. Wiegel, Beebe, and Moon (1957) [11] found no relation between these parameters in studies of ocean wave forces on cylindrical piles. Jen [4], in 1968, also failed to correlate C_m or C_d with Reynolds number in a laboratory study of a 6 inch diameter pile.

In 1958, Keulegan and Carpenter [5], investigating the inertia and drag coefficients on circular cylinders, found

a correlation between these force coefficients and a dimensionless parameter, V_mT/D. Working in a rectangular basin with standing waves, they covered V_mT/D values between 2.7 and 120 over a Reynolds number range from 4000 to 29,300. The lowest value of C_m and the highest value of C_d were found to occur at a V_mT/D of about 15.

Sarpkaya and Tuter [8], in 1974, with an oscillating U-shaped channel and various cylinders, reconfirmed Keulegan-Carpenter data except for a small spread in the upper regions of V_mT/D, where the Sarpkaya-Tuter data may be more accurate and reliable. An important finding of the Sarpkaya-Tuter work was that the lift or transverse force was as larage as the in-line force.

The close correlation between C_m and C_d and the period parameter V_mT/D is evidenced by the close fitting curves relating these parameters. The C_m curve of Kuelegan-Carpenter forms a lower envelope for ocean data gathered by Wiegal, Beebe, and Moon, while the C_d curve forms an upper limit for the same data [11].

The work on wave induced forces on cylinders has attracted much attention, but results seem quite scattered and sometimes contradictory. Also, the effect of a plane boundary in proximity to the cylinder presents a new variable. It is the purpose of this thesis to analyze the forces on a cylinder in the proximity of a plane wall and to correlate the various coefficients with the period parameter V_mT/D, and the relative

distance between the cylinder and the wall, through the use of harmonic motion.

II. METHOD OF ANALYSIS

To analyze the time dependent force in unsteady periodic flow, a Fourier analysis will be made, beginning with the Morison's equation given by

$$F=1/2\ C_d \rho A V|V| + C_m \rho \forall\ dV/dt \tag{9}$$

The enclosure of one of the components of V^2 term in "absolute value" brackets accounts for the change in sign of the resisting force as velocity changes direction in an oscillating flow.

For a circular cylinder, the equation reduces to:

$$F=C_m \pi/4 LD^2 \rho dV/dt + \frac{C_d}{2} LD\rho V|V| \tag{10}$$

Representing the velocity of the harmonic motion by

$$V=-V_m \cos\sigma t \tag{11}$$

and inserting into equation (10), one has

$$\frac{F}{\rho L V_m^2 D/2} = \frac{\pi^2 D}{V_m T} C_m \sin\sigma t - C_d |\cos\sigma t| \cos\sigma t \tag{12}$$

Multiplying both sides by sin t and integrating, one has,

$$\int_0^{2\pi} \frac{F \sin\sigma t\ d(\sigma t)}{\rho V_m^2 D/2\ .\ L} = \int_0^{2\pi} \frac{\pi^2 D}{V_m T} C_m \sin\sigma t \sin\sigma t\ d(\sigma t)$$

$$-\int_0^{2\pi} C_d |\cos\sigma t| \cos\sigma t | \sin\sigma t\ d(\sigma t) \tag{13}$$

which gives

$$\int_{o}^{2\pi} \frac{F \sin\sigma t \; d(\sigma t)}{\rho L V_m^{2} D/2} = \frac{\pi^{2} D \, C_m (\pi)}{V_m T} \tag{14}$$

and

$$C_m = \frac{2 \, V_m t}{\pi^{3} D} \int_{o}^{2\pi} \frac{F \sin\sigma t \; d(\sigma t)}{\rho L V_m^{2} D} \tag{15}$$

Multiplying both sides of the force equation by $\cos\sigma t$, and integrating, results in

$$\int_{o}^{2\pi} \frac{F}{\rho L V_m^{2} D/2} \cos\sigma t \; d(\sigma t) = \int_{o}^{2\pi} \frac{\pi^{2} D \, C_m}{V_m T} \sin\sigma t \cos\sigma t \; d(\sigma t) - \int_{o}^{2\pi} C_d |\cos\sigma t| \cos\sigma t \cos\sigma t \; d(\sigma t) \tag{16}$$

$$\int_{o}^{2\pi} \frac{F}{\rho L V_m^{2} D/2} \cos\sigma t \; d(\sigma t) = -8/3 \; C_d \tag{17}$$

Finally,

$$C_d = -3/4 \int_{o}^{2\pi} \frac{F \cos\sigma t}{\rho L V_m^{2} D} \, d(\sigma t) \tag{18}$$

For the analysis of these force coefficients a computer program was used (See Appendix A). The determination of V_m is made by considering the wave amplitude, A, and the period, T, resulting in

$$V_m = 2\pi A/T \tag{19}$$

Thus the coefficients C_m and C_d may be written as,

$$C_m = \frac{2T^2}{\pi^3 D^2 LA\rho} \Sigma F \sin\left(\frac{2\pi t}{T}\right) d(t/T) \tag{20}$$

$$C_d = \frac{-3T^2}{8\rho D\pi LA^2} \Sigma F\cos\left(\frac{2\pi t}{T}\right) d(t/T) \tag{21}$$

As an alternate method of computing the force coefficients, a least-squares method was also employed. The method of least squares consists of the minimization of the error between the measured and calculated forces. Letting F represent the instantaneous measured force and F_c the force calculated through the use of equation (10), and writing

$$E^2 = (F-F_c)^2 \tag{22}$$

and $dE^2/dC_m=0$ and $dE^2/dC_d=0$, one has

$$C_d = \frac{-8}{3\pi} \int_o^{2\pi} \frac{F|\cos\sigma t|\cos\sigma t}{\rho DLV_m^2} d(\sigma t) \tag{23}$$

and

$$C_m = \frac{2V_m T}{\pi^3 D} \int_o^{2\pi} \frac{F \sin\sigma t \, d(\sigma t)}{\rho V_m^2 LD} \tag{24}$$

It should be noted that the Fourier analysis and the method of least-squares yield identical C_m values and that the C_d values differ only slightly.

The error between the measured and calculated forces, particularly in the neighborhood of the maximum forces, may

be further minimized by choosing the square of the measured force as the weighting factor in the least-square analysis. Thus writing

$$E^2=F^2(F-F_c)^2 \tag{25}$$

and $dE^2/dC_d=0$ and $dE^2/dC_m=0$, one has

$$C_d=\frac{2}{\rho DLV_m^2}\,\frac{f_5f_3-f_4f_2}{f_4f_1-f_3f_3} \tag{26}$$

and

$$C_m=\frac{T^2}{\pi^3 LAD^2}\,\frac{f_5f_1-f_3f_2}{f_4f_1-f_3f_3} \tag{27}$$

The functions f_1 are given by

$$f_1=\int_0^{2\pi} F^2\cos^4\sigma t\; d(\sigma t) \quad , \quad f_2=\int_0^{2\pi} F^3|\cos\sigma t|\cos\sigma t\; d(\sigma t)$$

$$f_3=\int_0^{2\pi} F^2\sin\sigma t\,\cos\sigma t|\cos\sigma t|\,d(\sigma t) \tag{28}$$

$$f_4=\int_0^{2\pi} F^2\sin^2\sigma t\; d(\sigma t) \quad , \quad f_5=\int_0^{2\pi} F^3\sin\sigma t\; d(\sigma t)$$

Equations (27) and (28) may be shown to reduce to equations (23) and (24) by replacing F^n in equations (28) by F^{n-2} and carrying out the necessary integrations in which F does not appear.

Each wave cycle was divided into 36 time intervals of $\Delta t=2.86/36$ seconds, (T=2.86). The force for each interval was found and incorporated into the computer program to calculate

the appropriate coefficients through the use of the three methods of analysis cited above.

III. EXPERIMENTAL EQUIPMENT

The basic oscillating flow system consisted of a U-shaped vertical water channel with a channel cross section of 18 by 20 inches shown in Figure 1. Oscillations were created by pneumatic pressure applied at a closed end of the channel. The closed end was opened by means of a slider crank mechanism uncovering a large exit and releasing the air pressure. The resulting oscillation was a near perfect harmonic as evidenced by the elevation and acceleration traces shown in Figure 2.

The maximum amplitude of the oscillation was 11 inches and the natural damping of the oscillations was in the order of 1/8 inch per cycle. The water level at its minimum oscillation height was twenty inches above the test cylinder. The cylinders were manufactured out of plexiglass tubes or rods at desired diameters and at lengths approximately 1/16 inch less than the channel width. Self-aligning bearings were imbedded at each end of the cylinders and caution was taken before each experiment to confirm the clearance of the cylinder end from the channel walls.

The lateral and in-line (with respect to the fluid flow) force measuring devices consisted of various cantilever beams mounted to the ends of the test cylinder. Eight piezoresistive strain gauges were mounted on each cantilever beam and properly waterproofed.

These force transducers were repeatedly calibrated by hanging known loads at the midsection of the cylinder in the

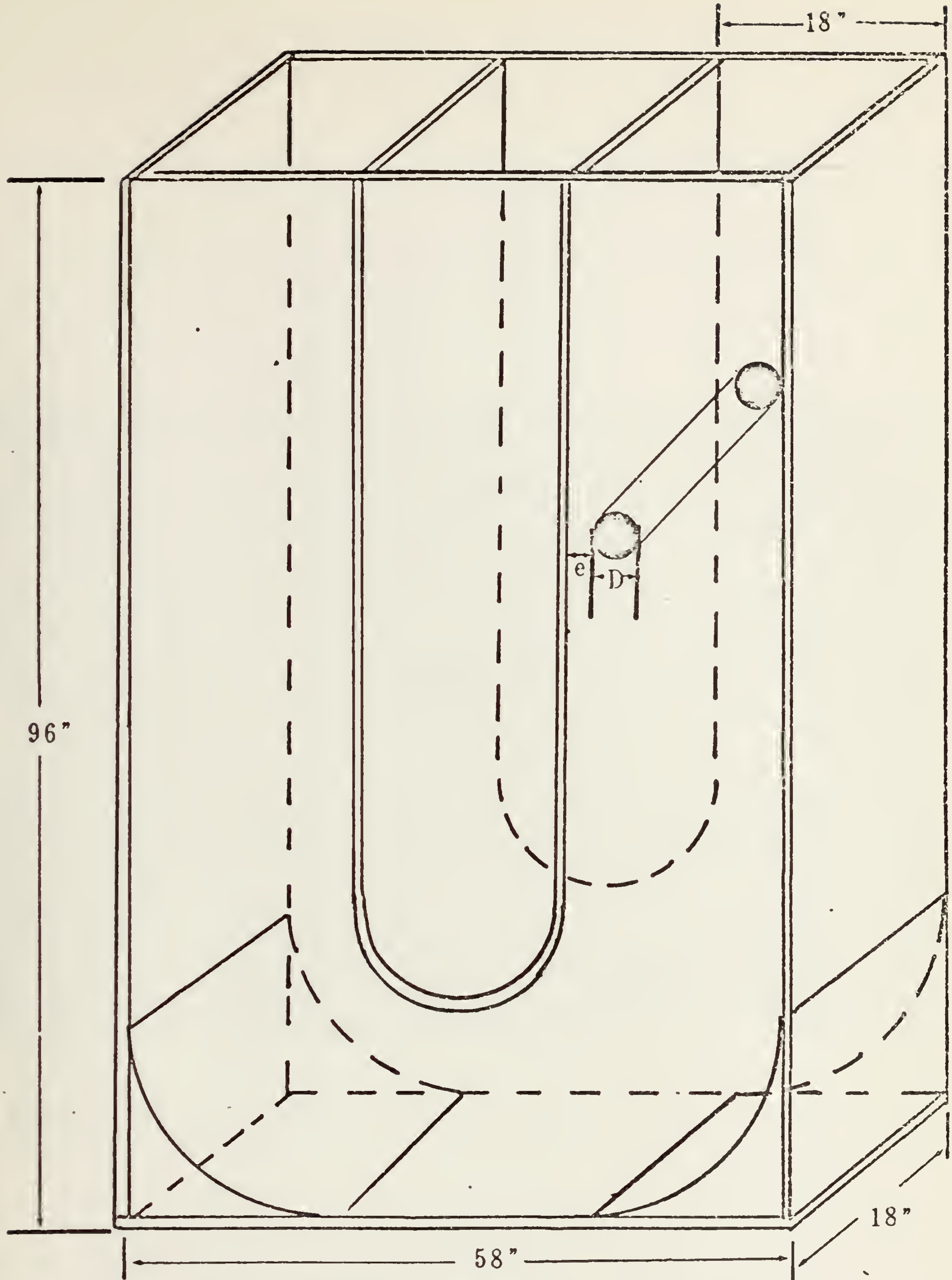

Fig. 1 Schematic drawing of the U-channel and cylinder orientation

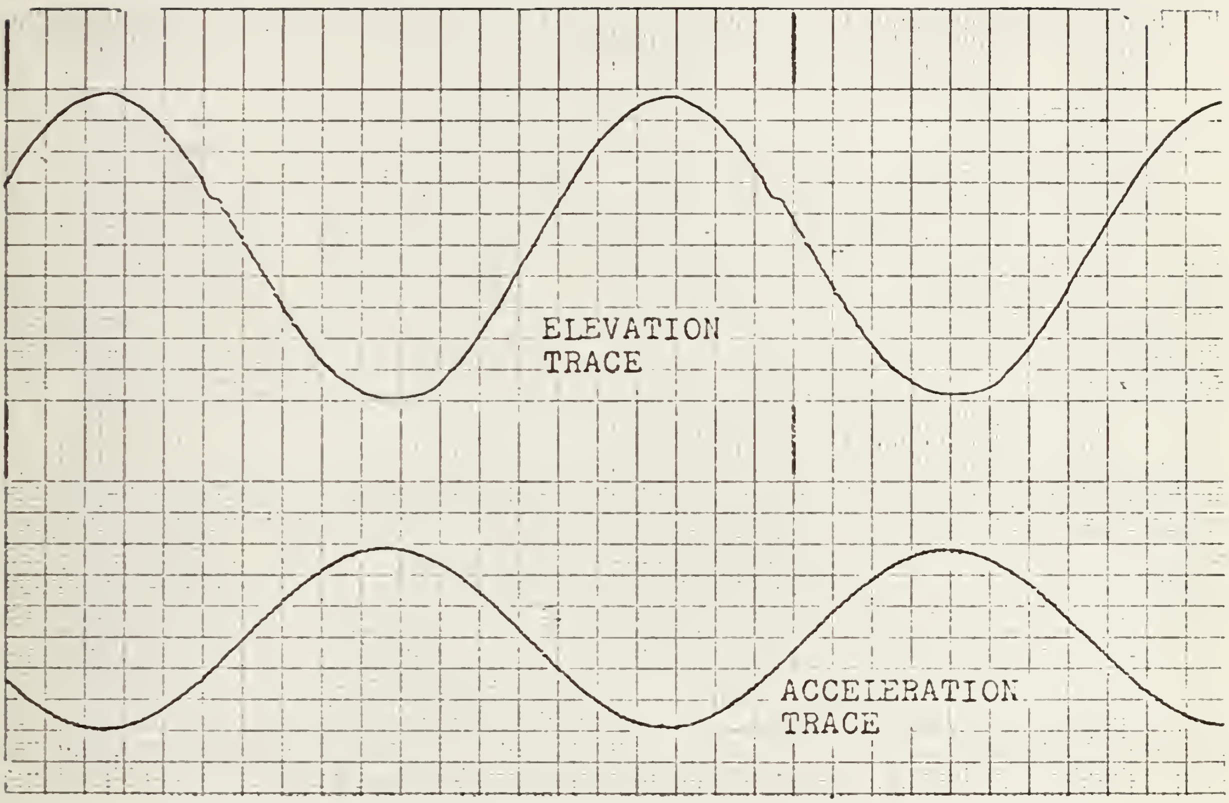

Fig. 2 Elevation and acceleration traces

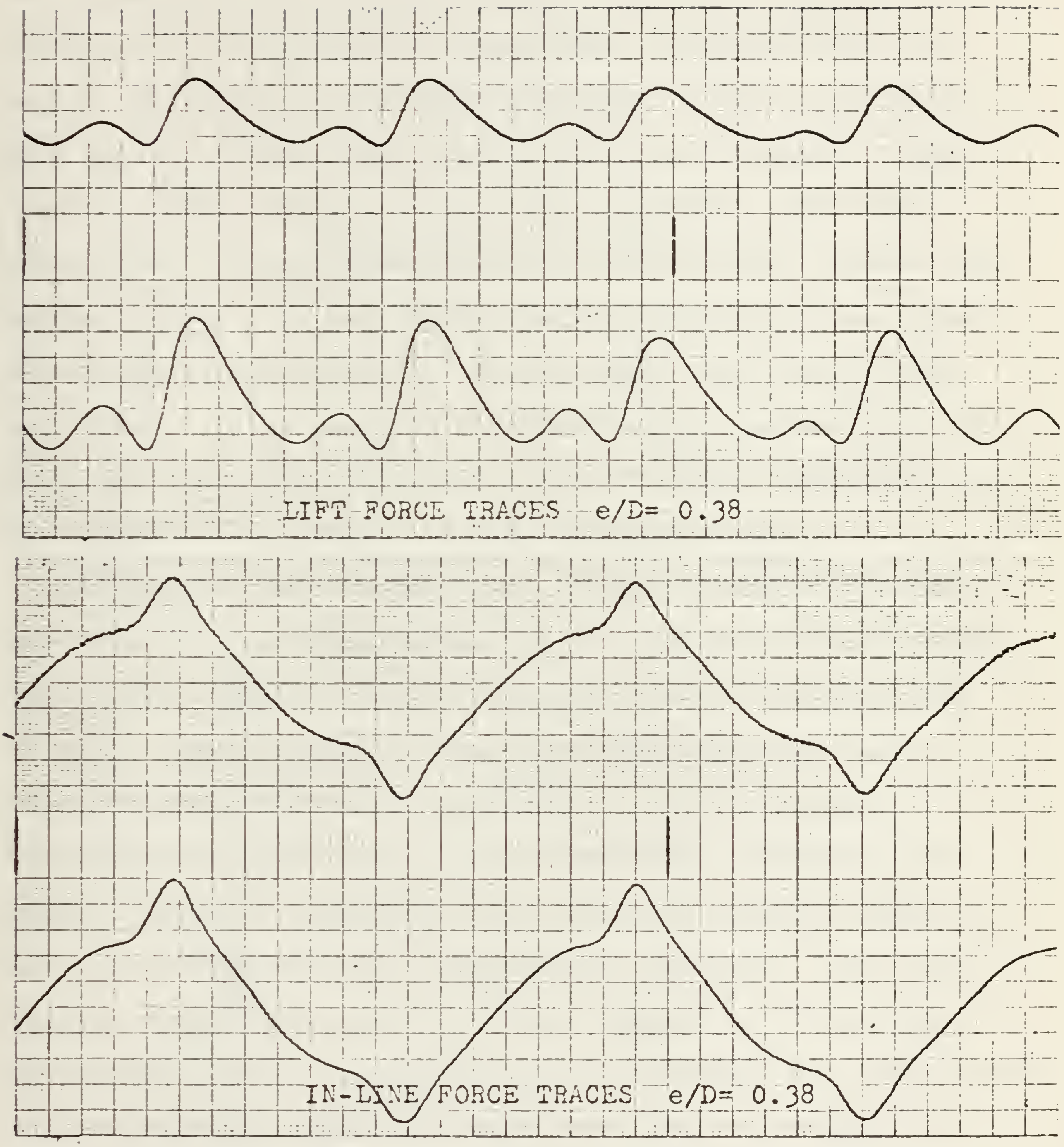

Fig 3. Force traces

horizontal and vertical directions. Some of the transducers were comprised of two pieces of thin cantilever beams cut orthogonal to each other and were able to measure both the in-line and lateral force simultaneously. Other transducers were capable of measuring only the in-line or lateral force. However, being rotatable $\pm 90°$, this transducer could first measure the in-line force and with a 90° rotation, measure the lateral forces. In many cases the in-line and lateral forces were measured at each end of the cylinder and compared with each other. In no case did the force curves deviate from each other more than 5%, indicating a fairly uniform response along the cylinder with respect to the resultant forces.

Throughout the investigation, the monitoring of the characteristics of the oscillations in the U-channel was of prime importance. Most of the difficulties in past determinations of C_m, C_d, and C_l resulted from the difficulty of producing a purely harmonic motion or from having to determine oscillation characteristics indirectly. The U-tube provides a perfectly sinusoidal oscillation and the instantaneous displacement and acceleration are continuously recorded. The instantaneous elevation in one leg of the channel was determined through the use of a capacitance wire connected to an amplifier-recorder system. Such wires have been used in the past to measure wave heights in open channels. The response of the wire was found through calibrations, to be perfectly linear within the range of oscillations encountered.

The instantaneous acceleration was measured by means of a differential-pressure transducer connected to two pressure taps at the mid-section of one of the channel walls. The acceleration was then calculated from

$$\Delta p = \rho s a_z \tag{29}$$

where ΔP is the differential pressure, ρ the fluid density, s the distance between pressure taps, and a_z the instantaneous acceleration.

The effect of pressure drop due to the viscous forces was found to be negligible.

The displacement and acceleration are, of course, in phase and may be used independently to calculate the velocity and displacement of the fluid, although displacement was actually used. The smoothness of the variation of acceleration and elevation traces shows the success in obtaining a purely harmonic motion as shown in Figure 2.

IV. DISCUSSION OF RESULTS

The drag coefficients are shown in Figure 4 as a function of the period parameter V_mT/D, which also equals $2\pi\underline{A}/D$, for various values of e/D. The actual data points are shown only for one value of e/D, partly to simplify the presentation of the data and partly to give some idea of the variation of C_d with respect to the three methods of analysis used in its evaluation. Firstly, it is apparent that all three methods yield nearly identical results and that the data exhibit very little scatter. Secondly, the drag coefficient can reach values as high as 3.75. For e/D larger than unity, C_d values approach those found for $V_mT/D=\infty$.

Evidently, it is not possible to explain the complex variations of C_d with V_mT/D since it is largely determined by separation effects.

The inertia coefficients are shown in Figure 5 in a manner similar to that for C_d. The values of C_m corresponding to $V_mT/D=0$ are obtained from the potential theory [10]. The experimental values approach in all cases those predicted by the potential theory as $V_mT/D \to 0$. Once again, the inertia coefficients approach those obtained for the limiting case of $e/D=\infty$ [8] for e/D values larger than unity.

The lift coefficients C_{lA} (force away from the wall) are shown in Figure 7 and the lift coefficients C_{lT} (force towards the wall) are shown in Figure 6. Also shown in Figure 6 are

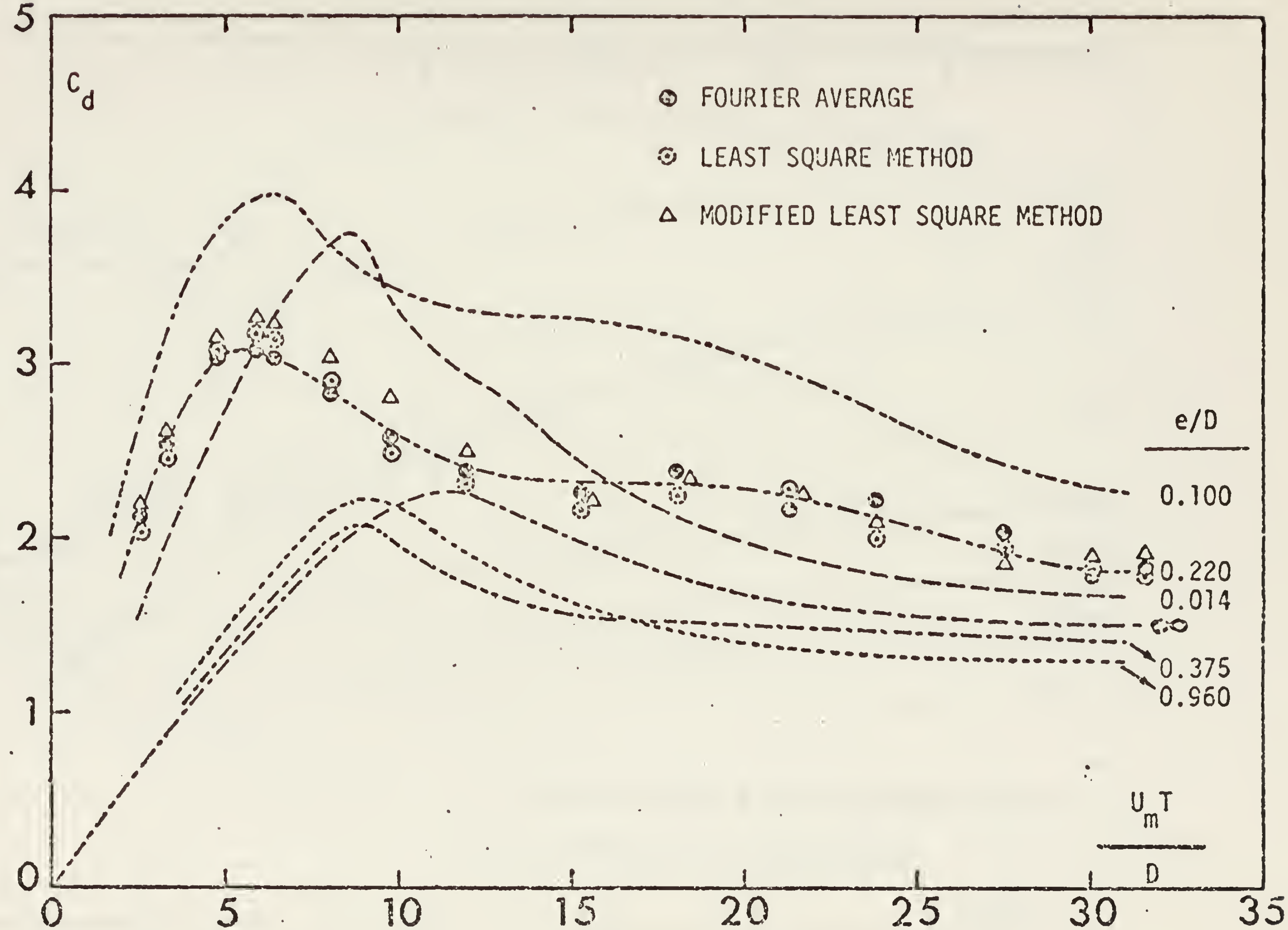

Fig.4 Drag coefficients versus period parameter

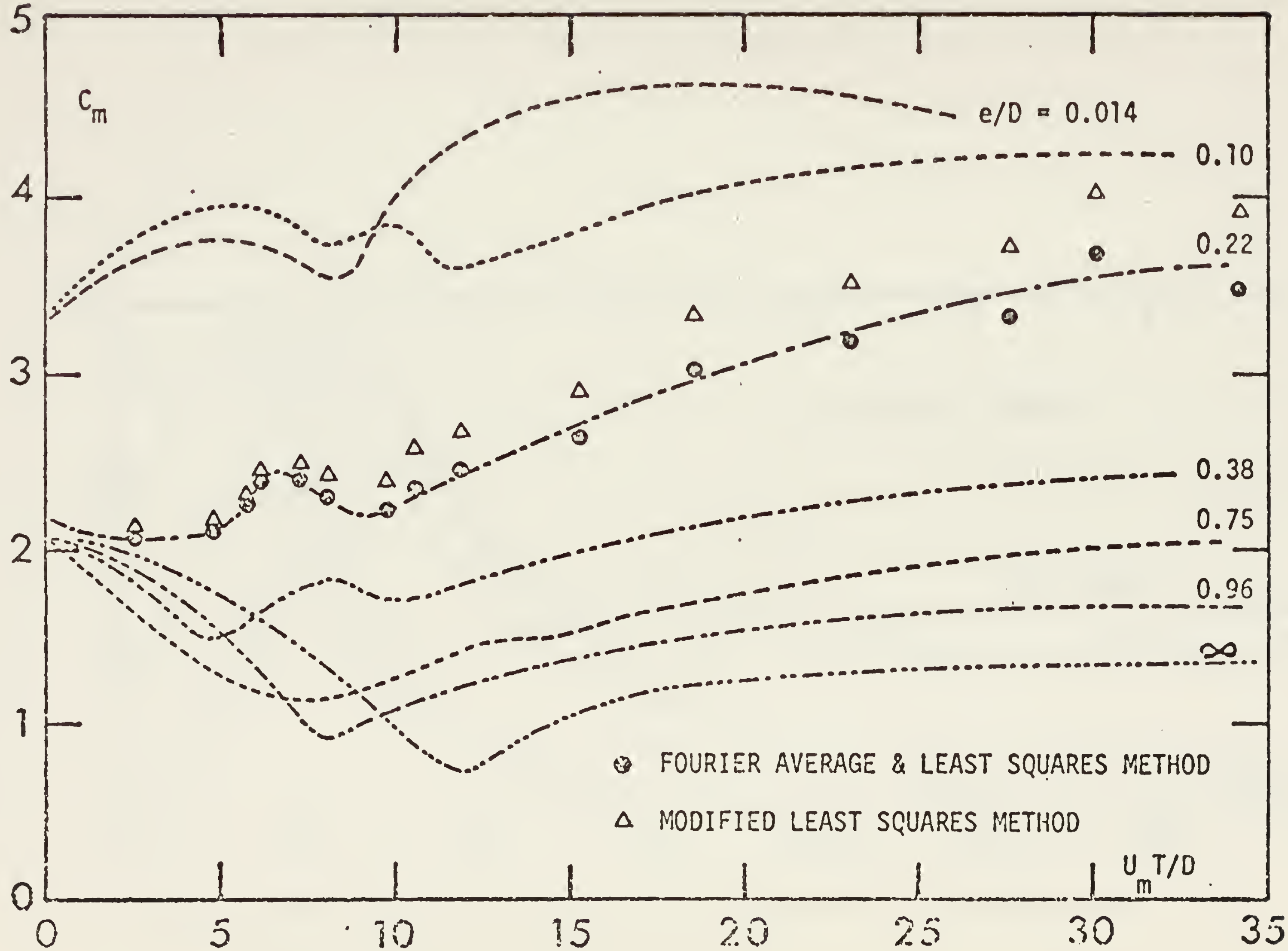

Fig.5 Inertia coefficients versus period parameter

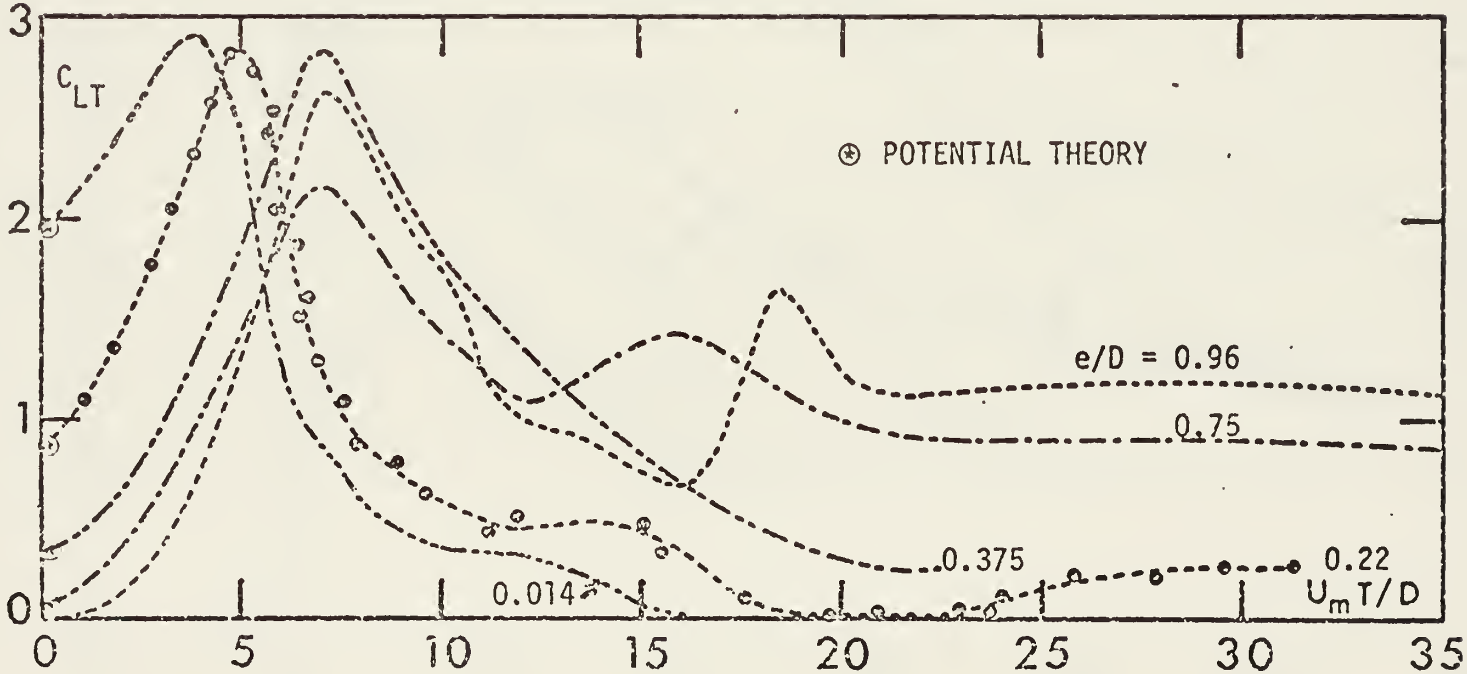

Fig.6 Lift coefficients versus period parameter
(force toward wall)

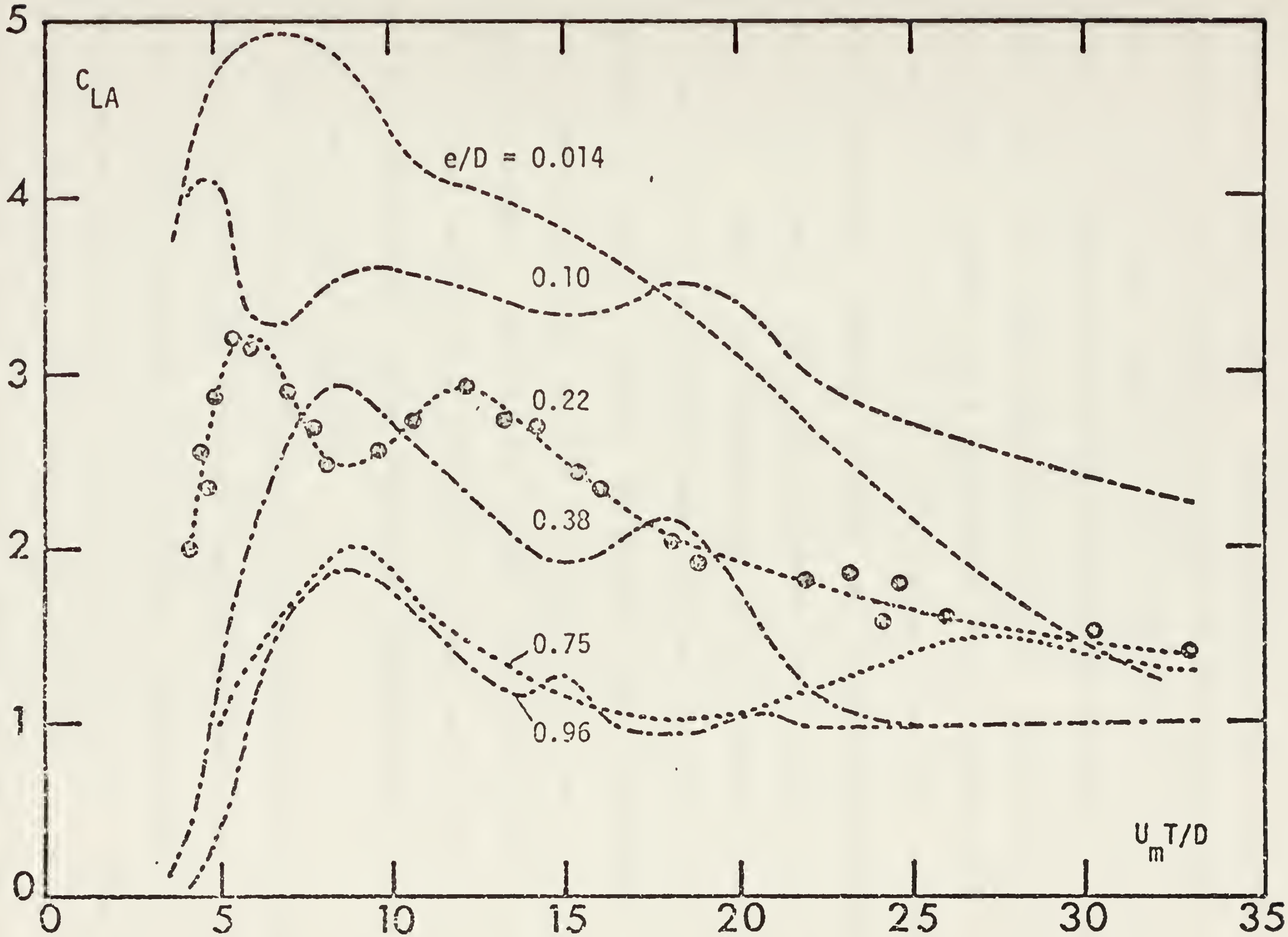

Fig.7 Lift coefficients versus period parameter
(force away from wall)

lift coefficients calculated through the use of the potential theory [10] for $V_mT/D=0$. Aside from the fact that the lift coefficients can become very large for cylinders near a wall, Figs. 6 and 7 also show that the predictions of the potential theory for separated flow may be grossly in error. Figure 7 shows that for a small gap (e/D=0.0143), large lift forces act on the cylinder in a direction away from the wall and C_{1T} is zero for all values of V_mT/D larger than 15. According to the potential theory, a large net force exists toward the wall when a small gap exists between the cylinder and the wall [10]. Thus, the predictions of the potential theory can be used only for extremely small values of V_mT/D for which separation does not occur. Evidently, the occurrence of separation depends not only on e/D and V_mT/D but also on the Reynolds number. No special effort has been made to determine the maximum values of V_mT/D for a given set of e/D values and Reynolds number below which the predictions of the potential theory may be applied.

The practical significance of the occurrence of large lift forces both away from and toward the wall in a given cycle of oscillation is self evident. Such alternating forces could give rise to large vertical oscillations. These oscillations can cause scour and fatigue and lead to larger inline forces than those calculated from equation (12) through the use of the coefficients from Figs. 4 and 5. In fact, it

is not difficult to imagine the occurrence of coupled in-line and transverse oscillations with disastrous consequences.

The frequency f_v of the alternating transverse force was evaluated in terms of the frequency f of the fluid oscillation and it was found, as done previously [8], that f_v is not a constant fraction of f and that several frequencies may occur during a given cycle. This seems to be rather reasonable because of the fact that in any cycle the magnitude of the velocity varies from zero to V_m and that there can hardly be a single Strouhal frequency. In spite of the multiplicity of the frequencies of vortex shedding, the examination of the force records have shown that the vortices are shed with significant regularity over most of the V_mT/D values at a dominant frequency of $f_v=2f$. Other frequencies of the alternating lift force were $f_v=f, 3f, 4f$, and $5f$.

Two additional matters need to be discussed, namely, the error between the measured and calculated in-line forces and the importance of the Reynolds number on the variation and correlation of the various force coefficients.

The relative error in each cycle for each V_mT/D as well as the error corresponding only to the maximum in-line force was calculated for each method of data analysis. The detailed results which will not be reported here for the sake of brevity have shown that λ defined by

$$\lambda = (F_{max}(\text{measured}) - F_{max}(\text{calculated}))/F_{max}(\text{calculated}) \quad (30)$$

is within $\pm 15\%$ and reaches its maximum in the neighborhood of $V_mT/D=10$ for the in-line force. This result may be taken as an indication of the fact that Morison's equation may be used to predict the in-line force acting on cylinders in the vicinity of a wall in a harmonically oscillating fluid through the use of the Fourier averaged coefficients.

As to the Reynolds number defined by V_mD/ν, its role in wave force coefficients is not well understood. For Reynolds numbers below the critical value (a value which is expected to be considerably smaller than that corresponding to the steady flow about a cylinder, partly due to unsteady nature of the flow and partly due to the presence of the vortices both upstream and downstream of the cylinder), the Reynolds number appears to play some role in the variation of C_d in the vicinity of the intermediate values of V_mT/D. For V_mT/D about 10, only one or two vortices form on the downstream side of the cylinder during a given cycle. As previously observed by Sarpkaya [9], when the fluid accelerates rapidly at high Reynolds numbers, vorticity is slow to diffuse and therefore accumulated rapidly in the growing separation bubble behind the cylinder. Although this bubble of trapped vorticity soon reaches unstable proportions, the growth of the bubble and, hence, of the resulting vortices, are so rapid that the

vortices become much larger than their quasi-steady-state size. Furthermore, the relatively slow diffusion of vorticity (largely due to turbulence rather than molecular diffusion) enables the vortices to retain a larger fraction of the vorticity shed from the boundary layers as the vortices move a small distance downstream before the flow is reversed. During this period, the drag on the cylinder rises above its steady-state value, both because the surface area covered by the separation bubble is temporarily greater than it would ultimately become in steady flow and because the enlarged wake distorts the outer flow, reducing the base pressure below its steady value. Thus, the effect of the Reynolds number, which is nearly absent in steady flow within the range of Reynolds numbers (4,000 to 30,000) discussed herein, is primarily due to the differences in the rate of shedding and diffusion of vorticity between the steady and periodic flow. However, the turbulent nature of diffusion and the excellent correlation of C_d with V_mT/D nearly obscure the effect of the Reynolds number, at least below the critical Reynolds number range. Near or above the critical Reynolds number range, however, the effect of the Reynolds number may become more pronounced due to different reasons. It must be kept in mind that C_d and C_m are time averages and the error between the measured and calculated forces through the use of these time-invariant coefficients is not uniform and depends on V_mT/D.

Similar arguments hold true for the transverse forces. The dependence of C_{lA} and C_{lT} on V_mT/D is much stronger and tends to obscure the weaker dependence on the Reynolds number.

V. CONCLUSIONS

Although the in-line and transverse forces acting on cylinders near a wall were measured for sinusoidally oscillating flow rather than for wave-type fluid motion, the results presented herein enable a number of conclusions concerning the latter type of flow to be drawn.

Morison's equation may be used to predict the in-line force acting on such cylinders or deeply submerged pipes (no free surface effects) subjected to local wave motion through the use of the Fourier averaged coefficients. The drag and inertia coefficients approach those predicted by the potentail theory as V_mT/D approaches zero.

The transverse forces, like the in-line forces, are strongly influenced by flow separation. Not only the magnitude but also the direction of the forces differ significantly from those predicted by the potential theory. For intermediate values of the period parameter, potential theory underestimates the transverse forces whereas for large values of V_mT/D, it grossly overestimates them.

Additional work with regard to the practical pipeline problems is needed to ascertain the effects of free surface, nonlinear waves, internal currents, roughness, and other environmental conditions. The data presented herein could form the basis for such extensions.

APPENDIX A

(IN-LINE FORCE COEFFICIENT PROGRAM)

```
CCCCCCCCCCCCCCCCCCCCCCCCCCCCCCCCCCCCCCCCCCCCCCCCCCCCCCCCCCCCCCCCCCCCCC
C                                                                    C
C      AVERAGE CD AND CM CALCULATIONS FOR CYLINDERS                  C
C                                                                    C
C      TIME=DIMENSIONLESS TIME (TIME/PERIOD)                         C
C      BETA=DIMENSIONLESS DISPLACEMENT (UMAX*PER/DIA)                C
C      AMP=AMPLITUDE OF MOTION IN FEET                               C
C      ZI=FORCE COEFFICIENTS                                         C
C      CM=INERTIA COEFFICIENT                                        C
C      PER=PERIOD IN SECONDS (CHART PERIOD/CHART SPEED)              C
C      CD=DRAG COEFFICIENT                                           C
C      REMF=REMAINDER FUNCTION                                       C
C      AI,BI=FOURIER COEFFICIENTS                                    C
C      N=NUMBER OF DATA SETS                                         C
C      CN=CONVERTION FACTOR                                          C
C                                                                    C
CCCCCCCCCCCCCCCCCCCCCCCCCCCCCCCCCCCCCCCCCCCCCCCCCCCCCCCCCCCCCCCCCCCCCC
       DIMENSION FORCE(36)
       N=5
       DO 100 I=1,N
       G=32.174
       READ(5,55) (FORCE(K), K=1,36)
       RHO=62.4/G
       PI=3.14159
       CNU=0.0000105
       CL=1.4946
C      INITIATE DATA SETS
C
C      READ IN PARAMETERS WHICH CHARACTERIZE THE DATA SET
C
       READ(5,10)DIA,AMP,PER,NCARD,UMX,CN,FMMM,NRUN
C
C      COMPUTE FORCE COEFFICIENTS
       Z1=(2*PER*PER)/(PI*PI*PI*DIA*DIA*CL*RHO*AMP)
       Z2=(-3*PER*PER)/(8*RHO*DIA*PI*CL*AMP*AMP)
       Z2LS=(-4*PER*PER)/(3*PI*PI*RHO*DIA*CL*AMP*AMP)
C      COMPUTE BETA
       BETA=2*PI*AMP/DIA
       REYNO=(UMX*DIA)/CNU
       WRITE(6,15)DIA,AMP,PER,UMX,CN,NRUN
       WRITE(6,20)
       TIME=0.0
       SUM=0.0
       DO 65 K=1,NCARD
       SUM=SUM+FORCE(K)
65     CONTINUE
       FMEAN=SUM/NCARD
       DO 85 K=1,NCARD
       FORCE(K)=FORCE(K)-FMEAN
85     CONTINUE
       FMMM=FMMM-FMEAN
       CM=0.0
       CD=0.0
       CMLS=0
       CDLS=0
       FAA=0.0
       FBB=0.0
       FCC=0.0
       FDD=0.0
       FEE=0.0
       DELTAT=0.027972028
       DO 200 K=1, NCARD
       F=CN*FORCE(K)
       ALPHA=2*PI*TIME
       SINA=SIN(ALPHA)
       COSA=COS(ALPHA)
       FSINA=DELTAT*F*SINA
       FCOSA=DELTAT*F*COSA
       FLS=DELTAT*F*COSA*ABS(COSA)
       FAAS=2*PI*F*DELTAT*COSA*COSA*COSA*COSA*F
       FBBS=2*PI*F*F*COSA*ABS(COSA)*DELTAT*F
       FCCS=2*PI*F*SINA*COSA*ABS(COSA)*DELTAT*F
```

```
      FDDS=2*PI*F*SINA*SINA*DELTAT*F
      FEES=2*PI*F*F*SINA*DELTAT*F
      FAA=FAAS+FAA
      FBB=FBBS+FBB
      FCC=FCCS+FCC
      FDD=FDDS+FDD
      FEE=FEES+FEE
      CM=FSINA+CM
      CD=FCOSA+CD
      CMLS=FSINA  +CMLS
      CDLS=FLS+CDLS
      WRITE(6,30)TIME,ALPHA,COSA,SINA,F,FCOSA,FSINA
      TIME=TIME+DELTAT
  200 CONTINUE
      CM=Z1*CM
      CD=Z2*CD
      CMLS=Z1*CMLS
      CDLS=Z2LS*CDLS
      CMFF=(Z1/2.0)*(FEE*FAA-FCC*FBB)/(FDD*FAA-FCC*FCC)
      CDFF=(-4.0*Z2/(3.0*PI))*(FEE*FCC-FDD*FB3)/(FDD*FAA-FCC
     *FCC)
      WRITE(6,35)
      WRITE(6,40)CM,CD,BETA,REYNO,CMLS,CDLS,CMFF,CDFF
      ANGLE=0.0
      WRITE(6,45)
      TIME=0.0
      DO 300 K=1,NCARD
      F=CN*FORCE(K)
      THETA1=((2.0*PI)/360)*ANGLE
      C1=(ABS(COS(THETA1)))*COS(THETA1)
      C2=RHO*((UMX**2.0)/2.0)*DIA*CL
      C3=((PI**2)*DIA*SIN(THETA1))/(UMX*PER)
      F1=(CM*C3-CD*C1)
      FLS=(CMLS*C3-CDLS*C1)
      FFOR=(CMFF*C3-CDFF*C1)
      F=F/C2
      REMF=ABS(F)-ABS(F1)
      FMAX=FMMM*CN/C2
      REMF=REMF/FMAX
      RLS=(ABS(F)-ABS(FLS))/FMAX
      RFOR=(ABS(F)-ABS(FFOR))/FMAX
      WRITE(6,50)TIME,F,F1,REMF,FLS,RLS,FFOR,RFOR
      ANGLE=ANGLE+10.06993
      TIME=TIME+DELTAT
  300 CONTINUE
  100 CONTINUE
   10 FORMAT(3F8.4,I8,3F8.4,I8)
   15 FORMAT('1',2X,'DIA=',F8.4,2X,'AMP=',F8.4,2X,'PER=',
     1F8.4,2X,'UMX=',F8.4,2X,'CN=',F8.4,2X,'NRUN=',I6)
   20 FORMAT('0',3X,'TIME/PER',7X,'ALPHA',7X,'COSA',15X,'SIN
     3',2X,'F',7X,'FCOSA',5X,'FSINA')
   30 FORMAT('0',3F12.4,F19.4,3F12.4)
   35 FORMAT('0',7X,'CM=',7X,'CD=',7X,'BETA=',7X,'REYNO=',7X
     1'CMLS=',7X,'CDLS=',7X,'CMFF=',7X,'CDFF=')
   40 FORMAT('0',6F12.4,2F12.4)
   45 FORMAT('0',7X,'TIME',9X,'F',9X,'F1',9X,'REMF',9X,'FLS'
     1'RLS',12X,'FFOR',12X,'RFOR')
   50 FORMAT('0',6F12.4,2F15.4)
   55 FORMAT(F10.4)
      STOP
      END
```

APPENDIX B

(LIFT COEFFICIENT PROGRAM)

```
CCCCCCCCCCCCCCCCCCCCCCCCCCCCCCCCCCCCCCCCCCCCCCCCCCCCCCCCCCC
C                           LIFT COEFFICIENTS                      C
C      H=GRAPHED WAVE HEIGHT (MM)                                  C
C      E=ELEVATION CALIBRATION (FT/MM)                             C
C      A=AMPLITUDE (FT)                                            C
C      D=CYLINDER DIAMETER (FT)                                    C
C      X=CYLINDER LENGTH (FT)                                      C
C      B=BETA (DIMENSIONLESS PERIOD PARAMETER)                     C
C      REYNO=REYNOLD'S NUMBER                                      C
C      UM=MAXIMUM WAVE VELOCITY  (FT/SEC)                          C
C      T=WAVE PERIOD (SEC)                                         C
C      FMU=GRAPHED FORCE AWAY FROM BOUNDARY(MM)                    C
C      FMD=GRAPHED FORCE TOWARDS BOUMDARY(MM)                      C
C      RHO=DENSITY (SLUGS/CUBIC FT)                                C
C      CLU=LIFT COEFFICIENT AWAY FROM BOUNDARY                     C
C      CLD=LIFT COEFFICIENT TOWARDS BOUNDARY                       C
C      ATTF=FORCE ATTENTUATION COEFFICIENT                         C
C      ATTA=AMPLITUDE ATTENUATION COEFFICIENT                      C
C      CN=FORCE CALIBRATION (LB/MM) AT ATTF=100                    C
CCCCCCCCCCCCCCCCCCCCCCCCCCCCCCCCCCCCCCCCCCCCCCCCCCCCCCCCCCCC
      WRITE(6,200)
      M=2
      DO 30 K=1,M
      READ (5,100) E,D,X,T,RHO,CN,N,J
      DO 20 I=1,N
      READ (5,400) H,ATTA,FMU,FMD,ATTF
      A=(H/2)*E*(ATTA/100)
      UM=2*3.1417*A/T
      B=UM*T/D
      REYNO=UM*D/0.0000105
      CLU=(FMU*ATTF*CN)/(.5*RHO*UM*UM*D*X*100)
      CLD=(FMD*ATTF*CN)/(.5*RHO*UM*UM*D*X*100)
      WRITE (6,300) J,D,B,REYNO,CLU,CLD
      J=J+1
20    CONTINUE
30    CONTINUE
100   FORMAT(6F8.4,I3,I3)
200   FORMAT(//,3X,'RUN #',4X,'DIAM',5X,'BETA',6X,'REYNO',5X
     ,'CLU',16X,'CLD,//)
300   FORMAT(//,4X,I2,6X,F6.4,3X,F5.2,4X,F8.1,3X,F6.4,2X,F6.
400   FORMAT(F8.4,F8.4,F8.4,F8.4,F8.2)
      STOP
      END
```

REFERENCES

1. Al-Kazily, M.F., "Forces on Submerged Pipelines Induced by Water Waves," Ph.D. Dissertation, College of Engineering, University of California, Berkeley, October 1972.

2. Arie, Mikio, Kiya, "Lift of a Cylinder in Shear Flow Subject to an Interference of a Plane Wall," Transactions of the Japan Society of Mechanical Engineers, Vol. 33, No. 246, February 1967.

3. Grace, R. A., "The Effect of Clearance and Orientation on Wave Induced Forces on Pipe Lines: Results of Laboratory Experiments," Technical Report No. 15, University of Hawaii-Look-LAB-71-15, April 1971.

4. Jen, Yaun, "Laboratory Study of Inertia Forces on Piles," Journal of the Waterways and Harbors Division, Proceedings of the ASCE, February 1968, pp. 59-76.

5. Keulegan, G. H., and Carpenter, L. H., "Forces on Cylinders and Plates in an Oscillating Fluid," Journal of Research, NBS, Vol. 60, 1958, pp. 423-440.

6. Morison, J. R., et al., "The Force Exerted by Surface Waves on Piles," Petroleum Transactions, AIME, Vol. 189, 1950, pp. 149-157.

7. Priest, M. S., "Wave Forces on Exposed Pipelines on the Ocean Bed," Paper No. OTC-1383, Third Annual Offshore Technology Conference, Houston, Texas, 1971.

8. Sarpkaya, T., "Forces on Cylinders and Spheres in a Sinusoidal Oscillating Fluid," Journal of Applied Mechanics, ASME, Vol. 42, Ser. E, No. 1, 1975, pp. 32-37.

9. Sarpkaya, T., "Separated about Lifting Bodies and Impulsive Flow About Cylinders," AIAA JOURNAL, Vol. 4, 1966, pp. 414-420.

10. Yamamoto, T., Nath, J. H., and Slotta, L. S., "Wave Forces on Cylinders Near Plane Boundary," Journal of the Waterways, Harbors and Coastal Engineering Div., ASCE, Vol. 100, No. WW4, pp. 345-359, November 1974.

11. Weigal, R. L., Oceanographical Engineering, Prentice-Hall, Inc., Englewood Cliffs, N. J., 1964.

12. Ralston, D. O., and Herbich, J. B., "The Effect of Waves and Currents on Submerged Pipelines," Texas Engineering Experiment Station, Coastal and Ocean Engineering Division, Report No. 101 - C.O.E., March 1968.

INITIAL DISTRIBUTION LIST

		No. Copies
1.	Defense Documentation Center Cameron Station Alexandria, Virginia 22314	2
2.	Library, Code 0212 Naval Postgraduate School Monterey, California 93940	2
3.	Department of Oceanography, Code 58 Naval Postgraduate School Monterey, California 93940	3
4.	Oceanographer of the Navy Hoffman Building No. 2 200 Stovall Alexandria, Virginia 22332	1
5.	Office of Naval Research Code 480 Arlington, Virginia 22217	1
6.	Dr. Robert E. Stevenson Scientific Liaison Office, ONR Scripps Institution of Oceanography La Jolla, California 92037	1
7.	Library, Code 3330 Naval Oceanographic Office Washington, D. C. 20373	1
8.	SIO Library University of California, San Diego P. O. Box 2367 La Jolla, California 92037	1
9.	Department of Oceanography Library University of Washington Seattle, Washington 98105	1
10.	Department of Oceanography Library Oregon State University Corvallis, Oregon 97331	1
11.	Fleet Numerical Weather Central Naval Postgraduate School Monterey, California 93940	1

12. Environmental Prediction Research Facility 1
Naval Postgraduate School
Monterey, California 93940

13. Department of the Navy 1
Commander Oceanographic System Pacific
Box 1390
FPO San Francisco 96610

14. Professor T. Sarpkaya, Code 59Dk 2
Department of Mechanical Engineering
Naval Postgraduate School
Monterey, California 93940

15. Assoc. Professor E. Thornton, Code 58Dk 1
Department of Oceanography
Naval Postgraduate School
Monterey, California 93940

16. Department Chairman, Code 59Nn 2
Department of Mechanical Engineering
Naval Postgraduate School
Monterey, California 93940

17. ENS Houston K. Jones, USN 1
2416 Morgan Court
Hobbs, New Mexico 88240

Thesis
J7223
c.1

160972

Jones
The effect of a plane boundary on wave induced forces acting on a submerged cylinder.